



## Robust depth control of a hybrid autonomous underwater vehicle with propeller torque's effect and model uncertainty

Huy Ngoc Tran <sup>a,b,\*</sup>, Thanh Nguyen Nhut Pham <sup>a</sup>, Sik Hyeung Choi <sup>c</sup>

<sup>a</sup> Faculty of Electrical & Electronics Engineering, Ho Chi Minh City University of Technology (HCMUT), 268 Ly Thuong Kiet Street, District 10, Ho Chi Minh City, Vietnam

<sup>b</sup> Vietnam National University Ho Chi Minh City, Linh Trung Ward, Thu Duc District, Ho Chi Minh City, Vietnam

<sup>c</sup> Department of Mechanical Engineering, Korea Maritime and Ocean University, Busan, Korea

### ARTICLE INFO

#### Keywords:

Autonomous underwater vehicle (AUV)  
Depth control  
Backstepping

### ABSTRACT

This paper presents a study of depth tracking controller design for a hybrid AUV in the presence of model uncertainty and propeller torque's effect. Firstly, the six degrees of freedom (6-DOF) nonlinear equations of motion, as well as the operating mechanisms and specific characteristics of the hybrid AUV, are described. Subsequently, the model for depth-plane is extracted by decoupling and linearizing the 6-DOF AUV model. Furthermore, a nonlinear disturbance observer (NDO) is constructed to deal with the linearization errors and uncertain components in the depth-plane model. A depth tracking controller is then designed based on the backstepping technique to guarantee the tracking error converges to an arbitrarily small neighborhood of zero. Besides, the robust stability of the proposed controller concerning the propeller torque's effect and the model uncertainty is analyzed. To ensure the objectivity and feasibility of the proposed method, the depth controller is applied to the 6-DOF model of AUV so that it maintains the coupling between roll, yaw, and pitch motion. Finally, the numerical simulation is carried out via MATLAB/SIMULINK to verify the controller's effectiveness, feasibility, and stability.

### 1. Introduction

Nowadays, autonomous underwater vehicles (AUV) have become a major tool for activities in deep sea because of the significant improvement in their performance. Specifically, in the scientific field is surveys, data collection and environmental sampling for hydrological research (Wynn et al., 2014; Eichhorn et al., 2018); in the military is clearing sea mines planted by enemies, conducting war activities with the navy (Hagen et al., 2003; Mondal et al., 2019); in the commercial field, AUVs are used to make detailed maps and surveys of the seafloor (oil and gas industries) before building subsea infrastructure (Mondal et al., 2019; Zhang et al., 2015). Therefore, research and development of controllers for AUV are essential.

In general, the controller design bases on the assumption that the model parameters are accurate. However, the model of AUV is a set of highly coupled nonlinear equations (Newman, 1977; Fossen, 1994) that lead to identifying completely accurate models (through estimation or empirical methods, etc.) is a difficult task. Besides, many control algorithms based on the linearization methods around the working point will

have a sharply reduced performance when either changing the model parameters or applying in practice. This can be seen through the comparison of simulation and experimental results in Naik and Singh (2007); Prestero (2001); Mahapatra and Subudhi (2018). Therefore, stability analysis and quality characterization surveys of the controller under the effect of model uncertainty is essential.

The control problem for AUV is a complex issue, so it is usually divided into three sub-problems for steering, diving and speed control (Jalving, 1994). In each sub-problem, it will be linearized to reduce interaction between each other, thereby simplifying the design of the controller. Consequently, AUV usually has three main controllers that are speed, steering, and diving controllers. In this paper, we only focus on studying the depth control problem (diving control problem) for AUV. For the depth control problem, in recent years, there have been many research projects showing the different algorithms applied to design the depth controller for AUV. For instance, with the simplest and most common algorithm, PID, there are Jalving (1994), Prestero (2001), Tanakitkorn et al. (2017). In Jalving (1994), after decomposing the AUV control into three subsystems, the PID controller was built for each

\* Corresponding author. Faculty of Electrical & Electronics Engineering of, Ho Chi Minh City University of Technology (HCMUT), 268 Ly Thuong Kiet Street, District 10, Ho Chi Minh City, Vietnam

system. For the depth controller, the mathematical model of depth-plane is established under the state-space form by linearizing and decoupling the motion model of AUV in the vertical plane. The pitch transfer function and the depth transfer function are then extracted from the state-space model to analyze. Then the parameters are selected to stabilize for the closed-loop transfer function of the whole system. In following the same approach as Jalving (1994), Prestero (2001) has developed a simple pitch-and-depth PD controller based on transfer functions derived from the linear state-space model. In Tanakitkorn et al. (2017), the PI-D scheme has been used to design the depth controller for Delphin2 AUV. This PI-D scheme has the derivative term fed by an actual state of the system instead of the tracking error to avoid the effect of the sudden change of setting value. The PI-D controller will make the system works more smoothly but this controller will not be able to process the time-varying desired signal. Moreover, the controller gain values are identified using a heuristic approach based on the Ziegler-Nichols method.

Besides linear controllers, nonlinear algorithms have also been studied and applied to AUV. Specifically, Hong et al. (2010), Joe et al. (2014), Yan et al. (2016), Tran et al. (2019) have developed various sliding mode control (SMC) algorithms for the depth-plane motion of AUVs. Hong et al. (2010) presented how to build an SMC controller and an experimental verification of it. This paper also addresses the effect of positive buoyancy in the dynamic model. Nevertheless, the author did not analyze the stability nor pointed out the advantages of the proposed control algorithm. In Joe et al. (2014), a second-order SMC was designed based on the 4-DOF diving model of AUV (ignore roll and pitch). The simulation and experiment were conducted on Cyclops AUV to verify the stability of the controller in the presence of parameter uncertainties and external disturbances. However, the internal stability of the closed-loop system was not guaranteed. An integral-fast terminal sliding mode control (IFTSMC) was explored by Yan et al. (2016) to control the AUV under the effect of parameter perturbations and wave disturbances. Notwithstanding, this paper only proves the convergence on the 3-DOF linear motion model of AUV in the vertical plane. Tran et al. (2019) proposed an indirect strategy to control depth for the hybrid AUV through pitch angle control. The simulation results show the simplicity and effectiveness of the proposed strategy. But the paper does not analyze the stability and performance of the controller when there are parameter uncertainties.

Moreover, several studies on backstepping techniques applied to depth control have been developed by Lapierre (2009), Cao et al. (2011), Wei et al. (2015), Gharesi et al. (2017), Mahapatra and Subudhi (2018). Lapierre (2009) proposed the adaptive controller and switching schemes to resolve external parameter uncertainty. In this paper, the adaptive laws were developed instead of the disturbance rejection to ensure the robustness. The simulation results show that the controller can handle when there are parameter uncertainties. However, the control performance isn't high, such as the response time is slow, the control signal is not smooth. Another backstepping controller combined with adaptive law to solve the parameter uncertainty and external disturbance was also discovered by Cao et al. (2011). Nevertheless, the controller design and verification simulation were based only on the 3-DOF model in depth-plane. Wei et al. (2015) formulated a linear state-space equation for vertical motion of AUV, then used backstepping techniques to build controllers. This paper addressed model uncertainties and developed a nonlinear disturbance observer (NDO) to deal with it. Similarly, a backstepping controller combines with a linear extended state observer (LESO) was design by Gharesi et al. (2017). Further, Mahapatra and Subudhi (2018) explored a depth control using the backstepping technique and nonlinear H-infinity technique. In this paper, random perturbations and uncertain hydrodynamic parameters were used to investigate the robustness of the proposed controller. The simulation and experiment results demonstrated the controller's effectiveness and feasibility, however, the control performance decline is proportional to the uncertainty magnitude.

Additionally, there exist other methods which are applied to control the depth of AUV. For example, a gain scheduling controller is proposed by Silvestre and Pascoal (2007) using a reduced output feedback technique for INFANTE AUV or the state-dependent Riccati equation (SDRE) technique developed in Naik and Singh (2007). Further, a constrained self-tuning controller based on Nonlinear Auto-Regressive Moving Average eXogenous (NARMAX) is utilized by Rout and Subudhi (2017) to track a given reference for a torpedo-shaped AUV. Besides, Yu et al. (2018) explores a sliding mode fuzzy control method combines with line-of-sight (LOS) guidance law to apply to a bioinspired robotic dolphin. Moreover, various  $H_\infty$  control methods have been developed for underwater vehicles by Liceaga-Castro and van der Molen (1995), Moreira and Soares (2008), Mahapatra et al. (2016), Mahapatra and Subudhi (2018). Similarly, the  $H_2$  optimal control methods applied to AUV in Moreira and Soares (2008), Wadoo et al. (2012), Qiao et al. (2018).

In general, the papers mentioned above often use linearizing and decoupling equations (3-DOF or 4-DOF) in the vertical motion of AUV for controller design, stability analysis, and simulation. It means that the coupling between roll, pitch, and yaw motion is neglected. Note that a torpedo-shaped AUV has a small moment of inertia and drag in the roll motion. Thus, the roll dynamic easily suffers oscillatory when the AUV is affected by propeller torque, unknown disturbances, yaw and pitch motion. Moreover, the roll motion is dynamically coupled into pitch motion so unwanted roll motion can reduce the diving performance and provide no clear opportunities for suppressing roll motion (Petrich and Stilwell, 2011). Besides, due to hydrodynamic characteristics, the motion equations of AUV are highly nonlinear and strongly coupled, so it is inevitable to have model uncertainties in the linear process. Therefore, it is necessary to investigate the robust stability and performance of the controller in the presence of propeller torque's effect and model uncertainties. On the other hand, the simulation model of AUV should be 6-DOF to ensure objectivity as well as the accuracy of the designed controller.

Motivated by the aforementioned analysis, this paper focuses on designing the nonlinear tracking controller for the vertical motion of a hybrid AUV. The control laws are produced by employing the backstepping technique to ensure stability and force the depth tracking error to an arbitrarily small neighborhood of zero, regardless of propeller torque's effect and model uncertainties. The designed controller is applied to a 6-DOF nonlinear model to ensure objectivity and feasibility. The simulation results will be specific evidence showing the efficiency, disturbances rejection ability, robustness, and superiority of the proposed method.

The remnant of this paper is organized as follows. Section 2 presents the AUV 6-DOF models, the operating mechanisms and specific characteristics of the hybrid AUV, and formulates control problem. Section 3 proposes the design of nonlinear disturbance observer (NDO) and backstepping controller for the depth-plane motion of the AUV and also analyzes the robust stability of the proposed controller under propeller torque's effect and model uncertainties. In Section 4, the numerical simulations and discussions are carried out to validates the previous analysis and design. Finally, the conclusions of this work are presented in Section 5.

## 2. AUV modelling and problem formulation

### 2.1. AUV modelling

The model will be considered in this paper is the AUV2000 mentioned in (Tran et al., 2019), AUV2000 shown in Fig. 1 is a hybrid AUV designed to integrate the outstanding characteristics of conventional AUV and underwater glider (a type of AUV that employs variable-buoyancy propulsion instead of traditional propellers or thrusters). Therefore AUV2000 can operate in two separate modes, specifically without using the thruster (Glider mode) and using the

thruster (AUV mode). However, in this paper, we only focus on designing the depth controller for AUV2000 in AUV mode.

### 2.1.1. Kinematics model

In accordance with SNAME (SNAME, 1950), the 6-DOF nonlinear kinematic and dynamic equations of motion of AUV are described in the earth-fixed frame  $\{e\}$  and the body-fixed frame  $\{b\}$  as shown in Fig. 2. According to Fossen, we have coordinate transform relating the translational velocities and the rotational velocities between  $\{b\}$  and  $\{e\}$  for various underwater vehicles in general and AUV in particular as follows:

$$\begin{cases} \begin{bmatrix} \dot{x} \\ \dot{y} \\ \dot{z} \end{bmatrix} = J_1(\eta_2) \begin{bmatrix} u \\ v \\ w \end{bmatrix} \\ \begin{bmatrix} \dot{\phi} \\ \dot{\theta} \\ \dot{\psi} \end{bmatrix} = J_2(\eta_2) \begin{bmatrix} p \\ q \\ r \end{bmatrix} \end{cases} \quad (1)$$

$$J_1(\eta_2) = \begin{bmatrix} \cos \psi \cos \theta & -\sin \psi \cos \varphi + \cos \psi \sin \theta \sin \varphi & \sin \psi \sin \varphi + \cos \psi \sin \theta \cos \varphi \\ \sin \psi \cos \theta & \cos \psi \cos \varphi + \sin \psi \sin \theta \sin \varphi & -\cos \psi \sin \varphi + \sin \psi \sin \theta \cos \varphi \\ -\sin \theta & \cos \theta \sin \varphi & \cos \theta \cos \varphi \end{bmatrix}$$

$$J_2(\eta_2) = \begin{bmatrix} 1 & \sin \varphi \tan \theta & \cos \varphi \tan \theta \\ 0 & \cos \varphi & -\sin \varphi \\ 0 & \frac{\sin \varphi}{\cos \theta} & \frac{\cos \varphi}{\cos \theta} \end{bmatrix}$$

where

$\eta_1 = [x \ y \ z]^T$ : the position of the vehicle with respect to  $\{e\}$

$\eta_2 = [\varphi \ \theta \ \psi]^T$ : the orientation (roll, pitch, yaw) of the vehicle with respect to  $\{e\}$

$v_1 = [u \ v \ w]^T$ : the translational velocities of the vehicle with respect to  $\{b\}$

$v_2 = [p \ q \ r]^T$ : the rotational velocities of the vehicle with respect to  $\{b\}$

### 2.1.2. Dynamic model of hybrid AUV

Following to (Prestero, 2001), the 6-DOF nonlinear dynamic equations of motion of AUV2000 can be expressed as

$$m[\ddot{u} - vr + wq - x_G(q^2 + r^2) + y_G(pq - \dot{r}) + z_G(pr + \dot{q})] = \sum X_{ext} \quad (2a)$$

$$m[\ddot{v} - wp + ur - y_G(r^2 + p^2) + z_G(qr - \dot{p}) + x_G(qp + \dot{r})] = \sum Y_{ext} \quad (2b)$$

$$m[\ddot{w} - uq + vp - z_G(p^2 + q^2) + x_G(rp - \dot{q}) + y_G(rq + \dot{p})] = \sum Z_{ext} \quad (2c)$$

$$I_{xx}\dot{p} + (I_{zz} - I_{yy})qr + m[y_G(\dot{w} - uq + vp) - z_G(\dot{v} - wp + ur)] = \sum K_{ext} \quad (2d)$$

$$I_{yy}\dot{q} + (I_{xx} - I_{zz})rp + m[z_G(\dot{u} - vr + wq) - x_G(\dot{w} - uq + vp)] = \sum M_{ext} \quad (2e)$$

$$I_{zz}\dot{r} + (I_{yy} - I_{xx})pq + m[x_G(\dot{v} - wp + ur) - y_G(\dot{u} - vr + wq)] = \sum N_{ext} \quad (2f)$$

where  $m$  is the AUV's mass,  $(x_G, y_G, z_G)$  is the center of gravity, and  $I_{xx}, I_{yy}, I_{zz}$  respectively are inertial moments about the x, y, and z axes. The

right side of equations (2a)-(2f) are the sum of the components of the force and moment acting on the vehicle:

$$\begin{aligned} \sum X_{ext} = & X_u\dot{u} + Z_wwq + Z_qq^2 - Y_vvr - Y_r r^2 + X_{u|u}|u|u| \\ & -(W - B)\sin \theta + X_{prop} \end{aligned} \quad (3a)$$

$$\begin{aligned} \sum Y_{ext} = & Y_v\dot{v} + Y_r\dot{r} + X_uur - Z_wwp - Z_qpq + Y_{v|v}|v|v| + Y_{r|r}|r|r| + Y_{uvl}uv \\ & +(W - B)\cos \theta \sin \varphi + Y_{rad} \end{aligned} \quad (3b)$$

$$\begin{aligned} \sum Z_{ext} = & Z_w\dot{w} + Z_q\dot{q} - X_uuq + Y_vvp + Y_r rp + Z_{w|w}|w|w| + Z_{q|q}|q|q| \\ & +(Z_{awl} + Z_{awf})uw + Z_{uaf}uq + (W - B)\cos \theta \cos \varphi \end{aligned} \quad (3c)$$

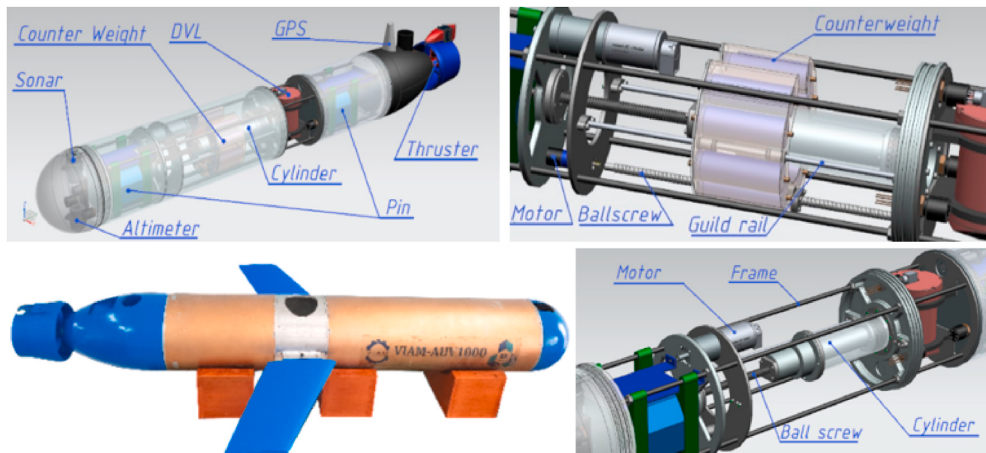


Fig. 1. AUV2000 prototype.

$$\begin{aligned} \sum K_{ext} = & K_p \dot{p} + (Z_{\dot{w}} - Y_{\dot{v}}) w v + (Z_{\dot{q}} + Y_{\dot{r}}) v q - (Z_{\dot{q}} + Y_{\dot{r}}) w r + (N_r \\ & - M_{\dot{q}}) q r + K_{p|p}|p|p| + (y_G W - y_B B) \cos \theta \cos \varphi \\ & - (z_G W - z_B B) \cos \theta \sin \varphi + K_{prop} \end{aligned} \quad (3d)$$

$$\begin{aligned} \sum M_{ext} = & Z_{\dot{q}} \dot{w} + M_{\dot{q}} \dot{q} - (Z_{\dot{w}} - X_{\dot{u}}) u w - Y_{\dot{v}} v p + (K_p - N_r) r p - Z_{\dot{q}} u q \\ & + M_{w|w}|w| + M_{q|q}|q| + (M_{uw} + M_{uw}) u w + M_{uq} u q \\ & - (z_G W - z_B B) \sin \theta - (x_G W - x_B B) \cos \theta \cos \varphi \end{aligned} \quad (3e)$$

$$\begin{aligned} \sum N_{ext} = & N_{\dot{v}} \dot{v} + N_{\dot{r}} \dot{r} - (X_{\dot{u}} - Y_{\dot{v}}) u v + Z_{\dot{q}} w p - (K_p - M_{\dot{q}}) p q + Y_{\dot{r}} u r \\ & + N_{v|v}|v| + N_{r|r}|r| + N_{uv} u v + (x_G W - x_B B) \cos \theta \sin \varphi \\ & + (y_G W - y_B B) \sin \theta + N_{rud} \end{aligned} \quad (3f)$$

In (3a)-(3f),  $X_{(.)}, Y_{(.)}, Z_{(.)}, K_{(.)}, M_{(.)}, N_{(.)}$  are the added mass, damping and lift terms,  $(x_B, y_B, z_B)$  is the center of buoyancy,  $W$  and  $B$  respectively are weight and buoyancy of AUV. The propeller force and torque are  $X_{prop}$  and  $K_{prop}$ , and the rudder force and moment are  $Y_{rud}$  and  $N_{rud}$ . In this paper, since we only concentrate on depth control, we will reduce  $Y_{rud}$ ,  $N_{rud}$  to zero in subsequent calculations.

### 2.1.3. The novel characteristic and operating mechanisms of AUV2000

As mentioned above, AUV2000 is a hybrid AUV that is designed to operate without using the thruster. Therefore, many structural elements resemble those of a typical underwater glider, the most significant of which are counterweight system and ballast system. In this section, the dissection of these operating mechanisms of AUV2000 is presented, thereby paving the way for the construction of the controller in the next section.

**2.1.3.1. Buoyancy engine dynamics analysis.** AUV2000 ballast system is a piston-cylinder which is arranged as shown in Fig. 3. Let  $V_{fix}$  be the volume occupied by AUV when the ballast system is full of water and  $\vec{r}_{fix} = [l_{fix}, 0, 0]^T$  be the current position of the center of buoyancy of AUV considered in the body-fixed frame. Moreover, denote  $V_{var}$  as the volume of water that the cylinder emits, then its relation to the position of the piston is formularized as

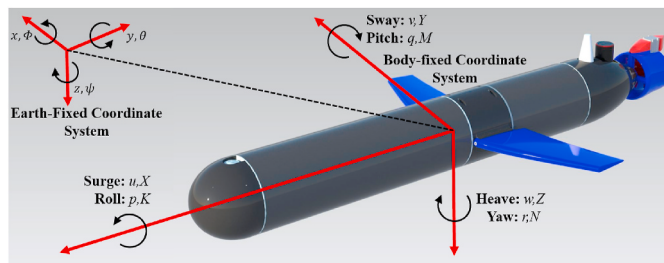


Fig. 2. AUV2000 body-fixed and earth-fixed coordinate systems.

$$V_{var} = S_c \cdot (l_c - x_p) \quad (4)$$

where  $S_c$  is the cross section of cylinder,  $l_c$  is the length of cylinder, and  $x_p$  is the piston position.

From Fig. 3 the formula for determining the buoyancy center of AUV can be expressed as

$$\vec{r}_{cb} = [x_B, 0, 0]^T = \left[ \frac{V_{var} \frac{l_c + x_p}{2} + V_{fix} l_{fix}}{V_{var} + V_{fix}}, 0, 0 \right]^T \quad (5)$$

and the buoyancy of AUV is:

$$B = \rho g (V_{fix} + V_{var}) \quad (6)$$

where  $\rho$  is the density of fluid,  $g$  is the gravitational acceleration.

**2.1.3.2. Analysis of the counterweight system.** Denote the total weight of AUV without counterweight (Fig. 4) as  $m_h$ , and let  $\vec{r}_h = [l_{hx}, l_{hy}, l_{hz}]^T$  be the mass center of  $m_h$  in the body-fixed frame. Because the counterweight's mass  $m_m$  is evenly distributed around the x-axis, the mass center of the counterweight in the body-fixed frame is  $\vec{r}_m = [x_m, 0, 0]^T$  where  $x_m$  is the counterweight position. As a result, the center of gravity of AUV can be determined by the following formula:

$$\vec{r}_{cg} = \frac{m_h \vec{r}_h + m_m \vec{r}_m}{m_h + m_m} = [x_G, y_G, z_G]^T = \left[ \frac{m_h l_{hx} + m_m x_m}{m_h + m_m}, \frac{m_h l_{hy}}{m_h + m_m}, \frac{m_h l_{hz}}{m_h + m_m} \right]^T \quad (7)$$

and the weight of AUV is:

$$W = mg = (m_h + m_m)g \quad (8)$$

**Remark 1.** Note that because  $\vec{r}_h$  is constant, it is evident from (7) that moving the counterweight only alters  $x_G$ . In other words,  $y_G$  and  $z_G$  are constant.

**Remark 2.** Like REMUS in (Prestero, 2001), to deal with propeller torque's effect, AUV2000's internal devices are arranged to obtain  $y_G, z_G$  so that the hydrostatic roll moment matches propeller torque, thus compensating for the roll offset. Therefore, by setting the number of revolutions (RPM) for the propeller to achieve the operating speed of AUV, the roll angle will be small and bounded during movement.

### 2.2. Problem formulation

In this paper, the objective is to develop a controller to maneuver the AUV tracking the desired depth in the vertical plane, notwithstanding of highly coupled model nonlinearities, propeller torque's effect, and model uncertainties. The objective can be divided into three sub-problems, as shown below.

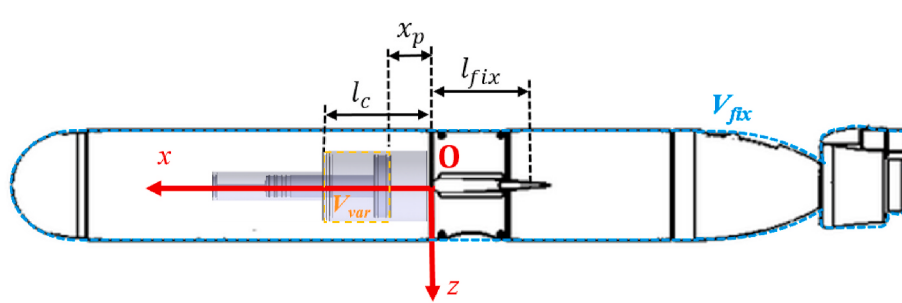
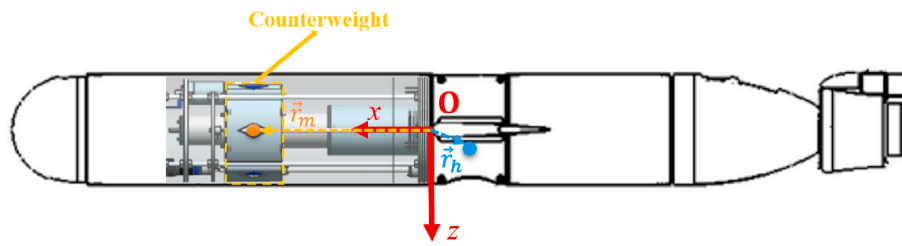


Fig. 3. Structure of the ballast system on AUV2000.



**Fig. 4.** Structure of the counterweight system on AUV2000.

- + Nonlinear disturbance observer (NDO) is employed to deal with linearization errors and model uncertainties in the depth-plane model.
- + Given a desired depth  $z_d$ , design a control law that determines the position of the counterweight based on the backstepping technique to guarantee the depth tracking error converges to an arbitrarily small neighborhood around zero as  $t$  goes to infinity, despite model uncertainties and propeller torque's effect.
- + The numerical simulations of the proposed controller applied to the 6-DOF AUV model are carried out to verify the disturbance resistance, robustness, and effectiveness of the developed control law.

### 3. Controller design

There exists various methods to build a depth controller for AUV, some of which are based on a state-space equation linearized from the depth-plane model ((Silvestre and Pascoal, 2007), (Naik and Singh, 2007), (Wei et al., 2015), (Gharesi et al., 2017)); transfer function (Jalving, 1994), (Prestero, 2001), (Qiao et al., 2018)); LOS in the vertical plane ((Tran et al., 2019), (Yu et al., 2018), (Rout and Subudhi, 2017)). This paper presents a different methodology to build a depth controller using the backstepping technique.

Before starting the design of the controller, it is noticeable that when the AUV operates without thruster, the ballast system no longer affects too much to the diving and floating process of AUV. Therefore, for convenience and simplicity, the paper will consider the ballast system with the volume to balance the buoyancy with the weight of AUV. Utilizing (6), (8) and (4) we can solve the position of piston to satisfy condition  $B = W$ .

From (1) we derive two differential equations for depth and pitch as follows:

$$\begin{cases} \dot{z} = -u \sin \theta + v \cos \theta \sin \varphi + w \cos \theta \cos \varphi \\ \dot{\theta} = q \cos \varphi - r \sin \varphi \end{cases} \quad (9a)$$

Further, combining (2e) and (3e), the nonlinear dynamic equation of pitch can be expressed as:

$$\begin{aligned} I_{yy}\dot{q} + (I_{xx} - I_{zz})rp + m[z_G(\dot{u} - vr + wq) - x_G(\dot{w} - uq + vp)] \\ = Z_q\dot{w} + M_q\dot{q} - (Z_w - X_u)uw - Y_vp + (K_p - N_r)rp - Z_quq \\ + M_{w|w|}w|w| + M_{q|q|}q|q| + (M_{uwl} + M_{uwf})uw + M_{uqf}uq \\ - (z_GW - z_B)\sin \theta - (x_GW - x_BB)\cos \theta \cos \varphi \end{aligned} \quad (10)$$

Performing linearization for equation (10) with  $\dot{u} = \dot{w} = p = v = r = \varphi = 0$  and note that  $z_B = 0$  from (5), we can obtain:

$$\begin{aligned} (I_{yy} - M_q)\dot{q} = (M_{uwl} + M_{uwf} - Z_w + X_u)uw + (M_{uqf} - Z_q)uq + M_{w|w|}w|w| \\ + M_{q|q|}q|q| - mz_Gwq - z_GW \sin \theta + x_BB \cos \theta \\ - (muq + W \cos \theta)x_G \end{aligned} \quad (11)$$

Now, from (10) and (11), we can derive pitch dynamic equation as following form:

$$\dot{q} = f_q + g_qx_G + d \quad (12)$$

where

$$f_q = \frac{\left[ (X_u - Z_w + M_{uwl} + M_{uwf})uw + (M_{uqf} - Z_q)uq + M_{w|w|}w|w| \right]}{I_{yy} - M_q}$$

$$g_q = -\frac{muq + W \cos \theta}{I_{yy} - M_q}$$

$d$  is the sum of the uncertain components of the model and the linearization errors.

Thereby, the depth-plane model can be expressed as

$$\begin{cases} \dot{z} = -u \sin \theta + v \cos \theta \sin \varphi + w \cos \theta \cos \varphi \\ \dot{\theta} = q \cos \varphi - r \sin \varphi \\ \dot{q} = f_q + g_qx_G + d \end{cases} \quad (13)$$

#### 3.1. NDO design

To estimate  $d$ , we define the new variable  $F = d - Lq$ , where  $L > 0$  is the observer gain which needs to be selected later. Then the nonlinear disturbance observer for  $d$  is constructed as follows:

$$\begin{cases} \hat{d} = \hat{F} + Lq \\ \dot{\hat{F}} = -L(f_q + g_qx_m + \hat{d}) \end{cases} \quad (14)$$

where  $\hat{d}$  and  $\hat{F}$  are the estimations of  $d$  and  $F$ , respectively. The estimated error is defined:

$$\tilde{d} = d - \hat{d}$$

and its derivative is:

$$\dot{\tilde{d}} = \dot{d} - \dot{\hat{d}} = \dot{d} - \dot{\hat{F}} - L\dot{q} = \dot{d} + L(f_q + g_qx_m + \hat{d}) - L(f_q + g_qx_m + d) = \dot{d} - L\tilde{d} \quad (15)$$

#### 3.2. Backstepping controller design

From here, we start building control laws by the backstepping technique and Lyapunov functions as follows:

**Step 1.** Let the desired depth be  $z_d$ , then the depth error can be defined as:

$$e = z - z_d, \quad (16)$$

Take the derivative of the depth error and utilizing (9a) yields:

$$\dot{e} = -u \sin \theta + v \cos \theta \sin \varphi + w \cos \theta \cos \varphi - \dot{z}_d \quad (17)$$

Define the first control Lyapunov function (CLF) as:  $V_1 := \frac{1}{2}e^2$  whose time derivative is

$$\dot{V}_1 = e\dot{e} = e \left( -u \sin \theta + v \cos \theta \sin \varphi + w \cos \theta \cos \varphi - \dot{z}_d \right)$$

The first virtual control law is selected as follows:

$$\begin{cases} \alpha = \theta - \theta_d & (18a) \\ \theta_d = \frac{k_1 e - \dot{z}_d}{U_0} & (18b) \end{cases}$$

where  $U_0$  is desired operating speed of AUV and  $k_1$  is the control gain which needs to be determined. Then the derivative of the first CLF can be expressed as:

$$\begin{aligned} \dot{V}_1 &= e \left( u(\theta - \sin \theta) - u\theta + v \cos \theta \sin \varphi + w \cos \theta \cos \varphi - \dot{z}_d \right) = ue(\theta - \sin \theta) + e \left( -u(\alpha + \theta_d) + v \cos \theta \sin \varphi + w \cos \theta \cos \varphi - \dot{z}_d \right) \\ &= ue(\theta - \sin \theta) - ue\alpha + e \left( -u \frac{k_1 e - \dot{z}_d}{U_0} + v \cos \theta \sin \varphi + w \cos \theta \cos \varphi - \dot{z}_d \right) = -\frac{u}{U_0} k_1 e^2 - ue\alpha + e \left( u(\theta - \sin \theta) + v \cos \theta \sin \varphi + w \cos \theta \cos \varphi \right. \\ &\quad \left. + \dot{z}_d \left( \frac{u}{U_0} - 1 \right) \right) \\ &= -\frac{u}{U_0} k_1 e^2 - ue\alpha + p_e \end{aligned} \quad (19)$$

$$\text{where } p_e = e \left( u(\theta - \sin \theta) + v \cos \theta \sin \varphi + w \cos \theta \cos \varphi + \dot{z}_d \left( \frac{u}{U_0} - 1 \right) \right) \quad (20)$$

**Step 2.** Differentiating (18a) with respect to time and utilizing (9b), we can obtain:

$$\dot{\alpha} = \dot{\theta} - \dot{\theta}_d = q \cos \varphi - r \sin \varphi - \dot{\theta}_d \quad (21)$$

Define the second CLF as:  $V_2 := V_1 + \frac{1}{2}\alpha^2$  whose time derivative is

$$\begin{aligned} \dot{V}_2 &= \dot{V}_1 + \alpha \dot{\alpha} = -\frac{u}{U_0} k_1 e^2 - ue\alpha + p_e + \alpha \left( q \cos \varphi - r \sin \varphi - \dot{\theta}_d \right) \\ &= -k_1 e^2 + \alpha \left( q \cos \varphi - r \sin \varphi - \dot{\theta}_d - ue \right) \end{aligned}$$

The second virtual control law is chosen as follows:

$$\begin{cases} \beta = q - q_d & (22a) \\ q_d = -k_2 \alpha + \theta_d + ue & (22b) \end{cases}$$

where  $k_2 > 0$  is control gain, hence

$$\begin{aligned} \dot{V}_2 &= -\frac{u}{U_0} k_1 e^2 + p_e + \alpha \left( (\beta + q_d) \cos \varphi - r \sin \varphi - \dot{\theta}_d - ue \right) \\ &= -\frac{u}{U_0} k_1 e^2 + p_e + \alpha \beta \cos \varphi + \alpha \left( q_d \cos \varphi - \sin \varphi r - \dot{\theta}_d - ue \right) \\ &= -\frac{u}{U_0} k_1 e^2 + p_e + \alpha \beta \cos \varphi + \alpha \left( (-k_2 \alpha + \dot{\theta}_d + ue) \cos \varphi - r \sin \varphi - \dot{\theta}_d - ue \right) \\ &= -\frac{u}{U_0} k_1 e^2 + p_e + \alpha \beta \cos \varphi - k_2 \alpha^2 + \alpha \left( (\dot{\theta}_d + ue) (\cos \varphi - 1) - r \sin \varphi \right) \end{aligned}$$

$$\text{Set } p_\alpha = p_e + \alpha \left( (\dot{\theta}_d + ue) (\cos \varphi - 1) - r \sin \varphi \right) \quad (23)$$

The second CLF can be rewritten as follows:

$$\dot{V}_2 = -\frac{u}{U_0} k_1 e^2 - k_2 \alpha^2 + p_\alpha + \alpha \beta \cos \varphi \quad (24)$$

**Step 3.** From (22a) and (12), the derivative of the second virtual control law can be derived as

$$\dot{\beta} = \dot{q} - \dot{q}_d = f_q + g_q x_G + d - \dot{q}_d \quad (25)$$

Consider the third CLF candidate:  $V_3 = V_2 + \frac{1}{2}\beta^2$  and its derivative is

$$\begin{aligned} \dot{V}_3 &= \dot{V}_2 + \beta \dot{\beta} = -\frac{u}{U_0} k_1 e^2 - k_2 \alpha^2 + p_\alpha + \alpha \beta \cos \varphi + \beta \left( f_q + g_q x_G + d - \dot{q}_d \right) \\ &= -\frac{u}{U_0} k_1 e^2 - k_2 \alpha^2 + p_\alpha + \beta \left( f_q + g_q x_G + d - \dot{q}_d + \alpha \cos \varphi \right) \end{aligned}$$

The control law is then designed as

$$x_G = \frac{-k_3 \beta - f_q + \dot{q}_d - \alpha - \hat{d}}{g_q} \quad (26)$$

where  $k_3 > 0$  and  $\hat{d}$  is the estimations of  $d$  which is feedback from NDO. Utilizing (25) and (7), the counterweight position can be determined. With the chosen control law, we obtain:

$$\begin{aligned} \dot{V}_3 &= -\frac{u}{U_0} k_1 e^2 - k_2 \alpha^2 + p_\alpha + \beta \left( f_q + g_q \frac{-k_3 \beta - f_q + \dot{q}_d - \alpha - \hat{d}}{g_q} - \dot{q}_d + \alpha \cos \varphi + d \right) \\ &= -\frac{u}{U_0} k_1 e^2 - k_2 \alpha^2 - k_3 \beta^2 + p_\alpha + \alpha \beta (\cos \varphi - 1) + \beta \tilde{d} \end{aligned}$$

$$\text{Let } p_\beta = p_\alpha + \alpha \beta (\cos \varphi - 1) \quad (27)$$

Then:

$$\dot{V}_3 = -\frac{u}{U_0} k_1 e^2 - k_2 \alpha^2 - k_3 \beta^2 + p_\beta + \beta \tilde{d} \quad (28)$$

**Step 4.** Define the fourth CLF as:  $V_4 = V_3 + \frac{1}{2}\tilde{d}^2$

Differentiating the fourth CLF and utilizing (15) yields

$$\begin{aligned} \dot{V}_4 &= \dot{V}_3 + \tilde{d} \dot{\tilde{d}} = -\frac{u}{U_0} k_1 e^2 - k_2 \alpha^2 - k_3 \beta^2 + p_\beta + \beta \tilde{d} + \tilde{d} (\dot{d} - L \tilde{d}) \\ &= -\frac{u}{U_0} k_1 e^2 - k_2 \alpha^2 - k_3 \beta^2 - L \tilde{d}^2 + p_\beta + \beta \tilde{d} + \tilde{d} \dot{d} \end{aligned}$$

Continue to set  $p_d = p_\beta + \beta \tilde{d} + \tilde{d} \dot{d}$

We get the final result as

$$\dot{V}_4 = -\frac{u}{U_0} k_1 e^2 - k_2 \alpha^2 - k_3 \beta^2 - L \tilde{d}^2 + p_d \quad (30)$$

### 3.3. Stability analysis

To facilitate the analysis of stability in the next step, the following assumptions are required:

**Assumption 1.** The model uncertainties and the linearization errors are bounded, so there exists a positive constant  $\Delta_d$  that satisfies  $|\dot{d}| \leq \Delta_d$ .

**Assumption 2.** The predefined desired depth is finite, such that  $|z_d|$ ,  $|\dot{z}_d|$ , and  $|\ddot{z}_d|$  are bounded. Thus, from (18b), it can be inferred that  $|\dot{\theta}_d|$  is

bounded, and we can set  $|\dot{z}_d| \leq \Delta_{zd}$  and  $|\dot{\theta}_d| \leq \Delta_{\dot{\theta}d}$ .

**Assumption 3.** Due to the mechanical properties of AUV2000 when designed, the pitch angle during operation will be bounded, specifically,  $|\theta| \leq 70^\circ$ . Therefore,  $|\theta - \sin \theta| \leq \frac{7\pi}{18} - \sin\left(\frac{7\pi}{18}\right)$ .

**Assumption 4.** The surge velocity  $u$  of AUV is non-negative and will converge to the vicinity of the desired operating speed  $U_0$  during movement (Jalving, 1994; Fossen, 1994; Prestero, 2001; Qiao et al., 2018). Let the maximum speed of AUV be  $u_{\max}$ , we have  $|u| \leq u_{\max}$  and  $\left|\frac{u}{U_0} - 1\right| \leq 1$ .

**Assumption 5.** The linear and angular velocities of AUV are bounded during operation. Hence, there exist the small positive constants  $\Delta_v$ ,  $\Delta_w$ , and  $\Delta_r$ , such that the following conditions is satisfied:  $|v \cos \theta \sin \varphi| \leq \Delta_v$ ,  $|w \cos \theta \cos \varphi| \leq \Delta_w$  and  $|r \sin \varphi| \leq \Delta_r$ .

Moreover, from Remark 2, it can be indicated that  $|\cos \varphi - 1| \leq \Delta_\varphi$  where  $\Delta_\varphi$  is a very small positive constant. From (20), (23), (27) and (29), we have:

$$\begin{aligned} p_d = & e \left( u(\theta - \sin \theta) + v \cos \theta \sin \varphi + w \cos \theta \cos \varphi + \dot{z}_d \left( \frac{u}{U_0} - 1 \right) \right) \\ & + \alpha \left( (\dot{\theta}_d + ue) (\cos \varphi - 1) - r \sin \varphi \right) + \alpha \beta (\cos \varphi - 1) + \beta \tilde{d} + \tilde{d} \dot{d} \end{aligned}$$

Utilizing these assumptions above, we can obtain:

$$\begin{aligned} p_d \leq & |e| \left( u_{\max} \left( \frac{7}{18}\pi - \sin \frac{7}{18}\pi \right) + \Delta_v + \Delta_w + \Delta_{zd} \right) + |\alpha| ((\Delta_{\dot{\theta}d} + u_{\max} |e|) \Delta_\varphi + \Delta_r) \\ & + |\alpha \beta| \Delta_\varphi + |\beta \tilde{d}| + |\tilde{d}| \Delta_d \end{aligned} \quad (31)$$

Let  $\Delta_e = u_{\max} \left( \frac{7}{18}\pi - \sin \frac{7}{18}\pi \right) + \Delta_v + \Delta_w + \Delta_{zd}$  and using the Young inequality, we get:

$$\begin{aligned} p_d \leq & |e| \Delta_e + u_{\max} |\alpha| |e| \Delta_\varphi + |\alpha| (\Delta_{\dot{\theta}d} \Delta_\varphi + \Delta_r) + |\alpha \beta| \Delta_\varphi + |\beta \tilde{d}| + |\tilde{d}| \Delta_d \\ \leq & \frac{e^2}{4\epsilon_1} + \epsilon_1 \Delta_e^2 + \left( \frac{\alpha^2}{4\epsilon_2} + \epsilon_2 e^2 \right) u_{\max} \Delta_\varphi + \frac{\alpha^2}{4\epsilon_3} + \epsilon_3 (\Delta_{\dot{\theta}d} \Delta_\varphi + \Delta_r)^2 + \left( \frac{\alpha^2}{4\epsilon_4} \right. \\ & \left. + \epsilon_4 \beta^2 \right) \Delta_\varphi + \epsilon_5 \beta^2 + \frac{1}{4\epsilon_5} \tilde{d}^2 + \frac{1}{4\epsilon_6} \tilde{d}^2 + \epsilon_6 \Delta_d^2 \end{aligned} \quad (32)$$

where  $\epsilon_i (i = 1, 2, 3, 4, 5, 6)$  are positive designed constants. Substituting (32) into (30) yields:

$$\begin{aligned} \dot{V}_4 \leq & - \left( \frac{u}{U_0} k_1 - \frac{1}{4\epsilon_1} - \epsilon_2 u_{\max} \Delta_\varphi \right) e^2 - \left( k_2 - \frac{u_{\max} \Delta_\varphi}{4\epsilon_2} - \frac{1}{4\epsilon_3} - \frac{\Delta_\varphi}{4\epsilon_4} \right) \alpha^2 - (k_3 \\ & - \epsilon_4 \Delta_\varphi - \epsilon_5) \beta^2 - \left( L - \frac{1}{4\epsilon_5} - \frac{1}{4\epsilon_6} \right) \tilde{d}^2 + \epsilon_1 \Delta_e^2 + \epsilon_3 (\Delta_{\dot{\theta}d} \Delta_\varphi + \Delta_r)^2 \\ & + \epsilon_6 \Delta_d^2 \end{aligned} \quad (33)$$

Then we can choose the control gains  $k_j (j = 1, 2, 3)$  that satisfy the following conditions:

$$\begin{aligned} \frac{u}{U_0} k_1 - \frac{1}{4\epsilon_1} - \epsilon_2 u_{\max} \Delta_\varphi > 0 \\ k_2 - \frac{u_{\max} \Delta_\varphi}{4\epsilon_2} - \frac{1}{4\epsilon_3} - \frac{\Delta_\varphi}{4\epsilon_4} > 0 \\ k_3 - \epsilon_4 \Delta_\varphi - \epsilon_5 > 0 \\ L - \frac{1}{4\epsilon_5} - \frac{1}{4\epsilon_6} > 0 \end{aligned} \Leftrightarrow \begin{cases} k_1 > \left( \frac{1}{4\epsilon_1} + \epsilon_2 u_{\max} \Delta_\varphi \right) \frac{U_0}{u} \\ k_2 > \frac{u_{\max} \Delta_\varphi}{4\epsilon_2} + \frac{1}{4\epsilon_3} + \frac{\Delta_\varphi}{4\epsilon_4} \\ k_3 > \epsilon_4 \Delta_\varphi + \epsilon_5 \\ L > \frac{1}{4\epsilon_5} + \frac{1}{4\epsilon_6} \end{cases} \quad (34)$$

Denote

$$\begin{cases} \rho := \min \left[ \left( \frac{u}{U_0} k_1 - \frac{1}{4\epsilon_1} - \epsilon_2 u_{\max} \Delta_\varphi \right), \left( k_2 - \frac{u_{\max} \Delta_\varphi}{4\epsilon_2} - \frac{1}{4\epsilon_3} - \frac{\Delta_\varphi}{4\epsilon_4} \right), \right. \\ \left. (k_3 - \epsilon_4 \Delta_\varphi - \epsilon_5), \left( L - \frac{1}{4\epsilon_5} - \frac{1}{4\epsilon_6} \right) \right] > 0 \\ \mu := \epsilon_1 \Delta_e^2 + \epsilon_3 (\Delta_{\dot{\theta}d} \Delta_\varphi + \Delta_r)^2 + \epsilon_6 \Delta_d^2 \end{cases} \quad (35)$$

From (33) and (35), it can be inferred that

$$\dot{V}_4 \leq -2\rho V_4 + \mu \quad (36)$$

Considering the tracking error vector that contains the error states of both the control and observer systems as follows:

$$\Omega := [e, \alpha, \beta, \tilde{d}]^T$$

The fourth CLF can be further derived as  $V_4 = \frac{1}{2} \|\Omega\|^2$ , which employing the Comparison Lemma in Khalil (2002), yields.

$$V_4(t) \leq V_4(0) e^{-2\rho t} + \frac{\mu}{2\rho} \text{ for } t \in [0, t_{final}]$$

Thus,

$$\|\Omega(t)\| \leq \|\Omega(0)\| e^{-\rho t} + \sqrt{\frac{\mu}{\rho}}, t \in [0, t_{final}] \quad (37)$$

equation (37) means that the tracking error vector remain in a bounded set around zero, which can be reduced by increasing  $\rho$  and decreasing  $\mu$ , in other words, by tuning the control and observer gain  $k_j (j = 1, 2, 3)$ ,  $L$  and choosing  $\epsilon_i (i = 1, 2, 3, 4, 5, 6)$ . Obviously, it can be concluded that the tracking error vector converges to a specified compact set around the origin with the estimated law in (14) and control laws in (18), (22), (26).

**Remark 3.** It is worth noting that the control laws (18), (22), and (26) do not contain the roll angle, thereby the control signal is independent of the variation of the roll rate and the roll angle during maneuvering. This makes the control signal smoother and more accessible to apply in practice.

### 4. Simulation results

This section presents the numerical simulations of the proposed controller apply to AUV2000 on Matlab/Simulink. By analyzing the simulation results, the effectiveness, feasibility, and stability of the proposed method are clarified. In this study, the desired operating speed of the vehicle is considered to be  $U_0 = 1.28(m/s)$ . The control and observer gains selected for the controller are  $k_1 = 3, k_2 = 7.5, k_3 = 0.15, L = 5$ . To ensure objectivity and completeness, in these simulations, the vehicle is expected to track different desired paths in the vertical plane. Besides, the initial condition of the AUV considered for all simulation is as follows:

$$\begin{cases} [x, y, z, \varphi, \theta, \psi]^T = [0, 0, 0, 0, 0, 0]^T \\ [u, v, w, p, q, r]^T = [0, 0, 0, 0, 0, 0]^T \end{cases}$$

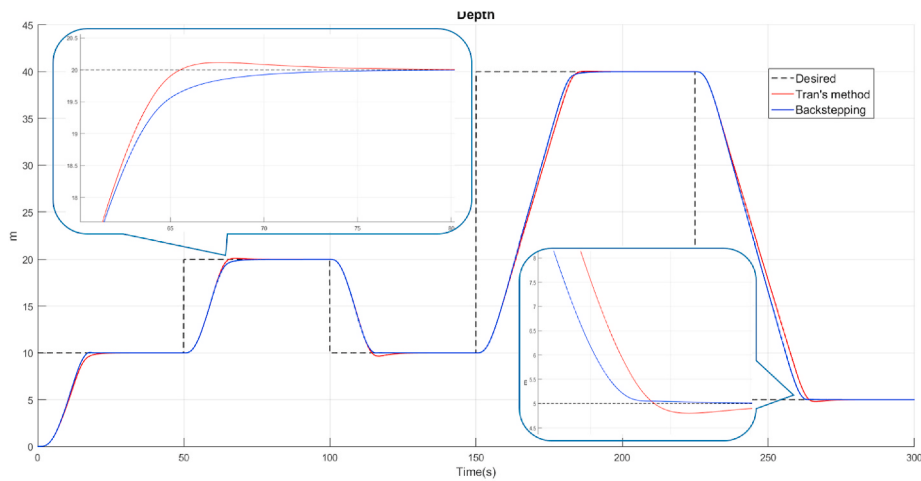


**Fig. 5.** The depth response when the desired depth is constant by the proposed controller (blue solid line) and the controller in Tran et al. (2019) (red solid line) with desired depth (black dotted line). (For interpretation of the references to colour in this figure legend, the reader is referred to the Web version of this article.)

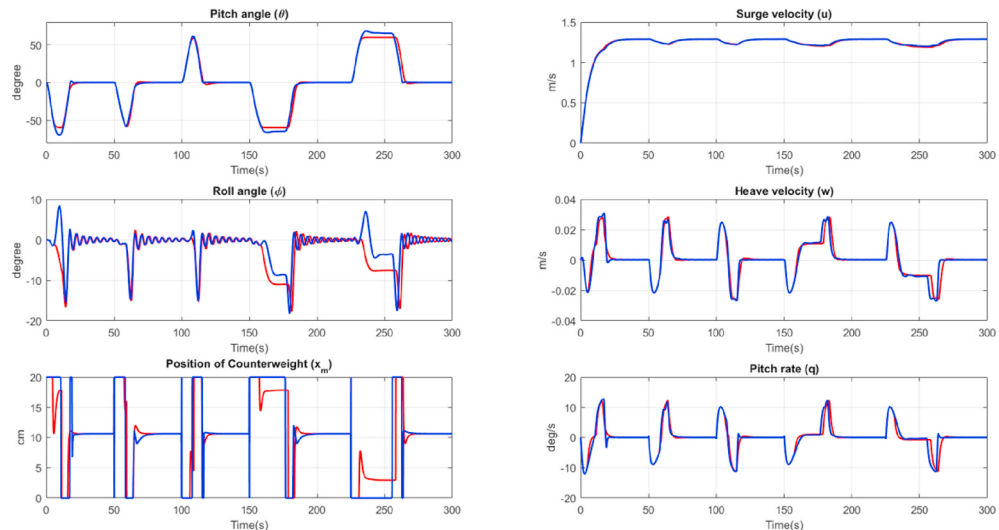


**Fig. 6.** The state response of AUV2000 when the desired depth is constant by the proposed controller (blue solid line) and the controller in Tran et al. (2019) (red solid line). (For interpretation of the references to colour in this figure legend, the reader is referred to the Web version of this article.)

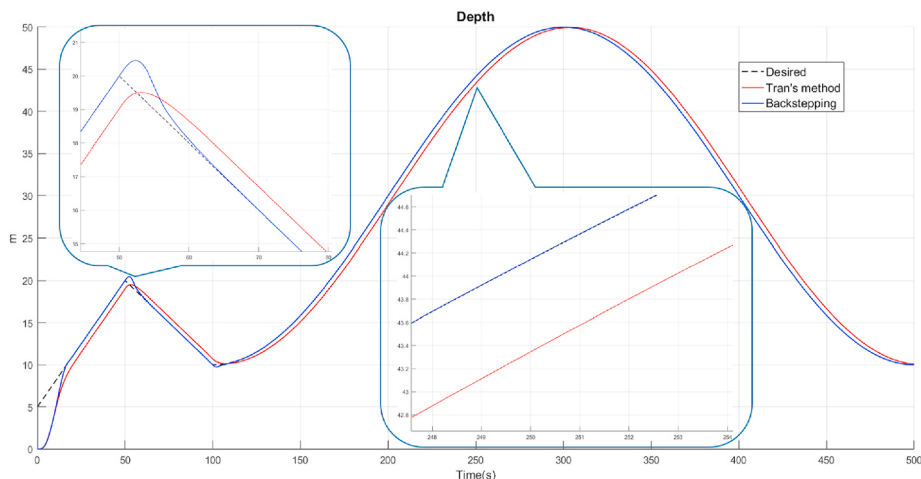


**Fig. 7.** The depth response with the composite desired depth by the proposed controller (blue solid line) and the controller in Tran et al. (2019) (red solid line). (For interpretation of the references to colour in this figure legend, the reader is referred to the Web version of this article.)

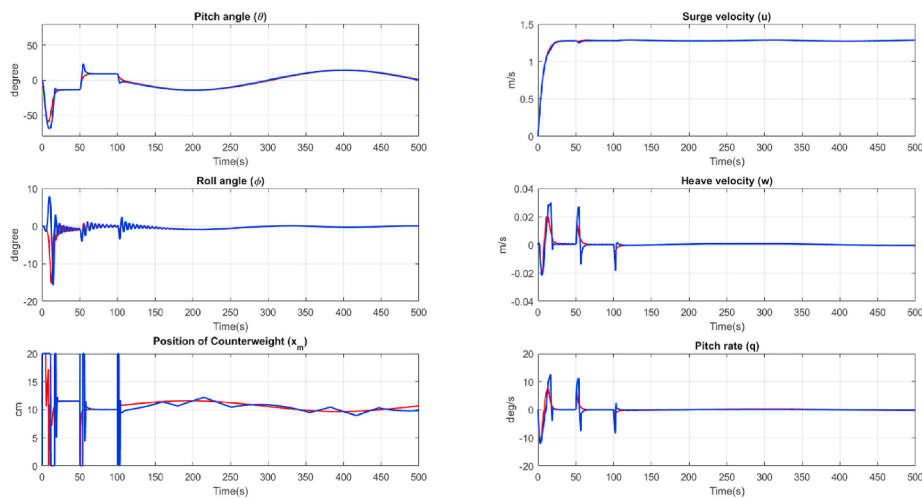


**Fig. 8.** The state response of AUV2000 with the composite desired depth by the proposed controller (blue solid line) and the controller in Tran et al. (2019) (red solid line). (For interpretation of the references to colour in this figure legend, the reader is referred to the Web version of this article.)

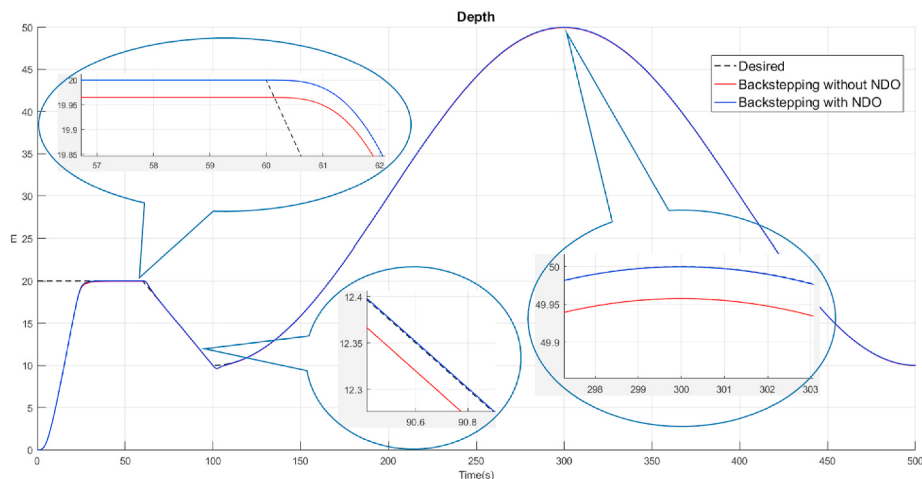


**Fig. 9.** The depth response with the composite desired depth by the proposed controller with NDO (blue solid line) and without NDO (red solid line) in the presence of the model uncertainties. (For interpretation of the references to colour in this figure legend, the reader is referred to the Web version of this article.)

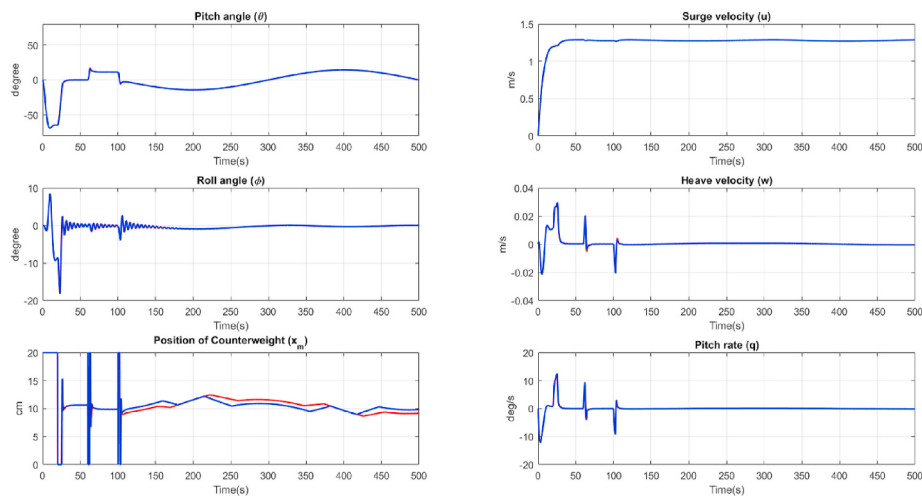


**Fig. 10.** The state response of AUV2000 with the composite desired depth by the proposed controller with NDO (blue solid line) and without NDO (red solid line) in the presence of the model uncertainties. (For interpretation of the references to colour in this figure legend, the reader is referred to the Web version of this article.)

#### 4.1. Simulations in the absence of the model uncertainties

Because of the similarity when using the nonlinear algorithm to build the controller for AUV2000, the comparison of control performances are constructed between the proposed backstepping controller and the controller developed in [Tran et al. \(2019\)](#).

##### 4.1.1. The desired depth is constant

[Fig. 5](#) shows that both the Tran's controller and the backstepping controller perform consistently with the 6-DOF model, not only speeding up the convergence process of the vehicle to the desired depth but also stabilizing the equilibria. However, the proposed backstepping controller has better control performance, such as no overshoot and faster convergence. Because [Fig. 6](#) shows the pitch angle during maneuvering is always within the limit (smaller than 70°), this ensures that the AUV will not fall into a singular point. Moreover, the roll angle overshoots when counterweight displaces abruptly then recovers to an equilibrium. Therefore, it indicates that the proposed controller can operate consistently, even when including the involvement of the roll angle, roll rate, sway velocity, yaw rate.

##### 4.1.2. The desired depth is not constant ( $\dot{z}_d \neq 0$ )

In this case study, we examine the composite desired depth, which is a combination of three scenarios as follows: 1)  $z_d = 5 + 0.3t$ , ( $0 \leq t < 50$ ); 2)  $z_d = 30 - 0.2t$ , ( $50 \leq t < 100$ ); 3)  $z_d = 30 - 20 \cos(0.005\pi t - 0.5\pi)$ , ( $t \geq 100$ ). The results in [Fig. 7](#) illustrate the disadvantage of most classical controllers ([Prestero, 2001](#); [Tanakitkorn et al., 2017](#); [Tran et al., 2019](#); [Qiao et al., 2018](#)) that it is incapable of making the vehicle converge on the desired depth when the desired depth is not constant. Meanwhile, the proposed controller not only ensures excellent tracking performance for AUV but also keeps AUV's roll angle in a bounded set around zero, as shown in [Fig. 8](#).

Through all the simulation results above, the proposed method has proved its superiority compared to the previous ones because it enables AUV to track straight lines, even with the curve paths. Besides, the tracking error always converges to zero and has fast convergence speed (about 20 s) with many different simulation conditions, thus the efficiency and stability of the proposed control law are verified. Moreover, it is easily observed that the velocity  $u$  is changed when the pitch angle alters, thereby using  $U_0$  in the controller design instead of using  $u$  in formula (18b) delivers the control signal smoother without affecting the system stability.

#### 4.2. Simulations in the presence of the model uncertainties

To evaluate the controller's robustness, [Joe et al. \(2014\)](#) varied the hydrodynamic coefficients by 20% to their actual values, [Qiao et al. \(2018\)](#) and [Mahapatra and Subudhi \(2018\)](#) considered the uncertainties of the model parameters by 20–25% and 30% of its nominal value, respectively. In this paper, to verify the disturbance resistance and robustness of the proposed controller, the parameters of  $f_q$  and  $g_q$  in formula (12) deviate by 30–40% from their accurate value.

In [Fig. 9](#), the desired depths of several scenarios are as follows: 1)  $z_d = 20$ , ( $0 \leq t < 60$ ); 2)  $z_d = 35 - 0.25t$ , ( $60 \leq t < 100$ ); 3)  $z_d = 30 - 20 \cos(0.005\pi t - 0.5\pi)$ , ( $t \geq 100$ ). It is noticeable from [Fig. 9](#) that the proposed controller still works without NDO, yet it suffers from a small steady-state error. Besides, [Fig. 10](#) shows that there is hardly any difference in the state variables of the two controllers. These simulation results sufficiently validate the strong robustness of the backstepping controller. In addition, the proposed controller is combined with NDO to compensate for the systematical parametric uncertainties, thereby eliminating the steady-state error and maintaining the control performance. In conclusion, the outstanding characteristics of the proposed controller are preserved despite the presence of the model uncertainties and propeller torque's effect.

## 5. Conclusion

The paper provides a new approach to building the depth tracking controllers for AUV2000 - a hybrid AUV type. The proposed controller has been applied to the 6-DOF AUV model to ensure nonlinearity and strongly coupled in the motion equations as well as a feasibility study for practical applications. The paper also considered the effect of roll angle and model uncertainty on the controller and proved the stability of the developed controller. The numerical simulations have been carried out and validated to verify the effectiveness and robustness of the proposed method. Moreover, the simulations results demonstrate the proposed control law has superior performance to previous ones and solves the depth control problem more fully for the depth tracking problem in the presence of the model uncertainties and propeller torque's effect.

## Declaration of competing interest

The authors declare that they have no known competing financial interests or personal relationships that could have appeared to influence the work reported in this paper.

## Acknowledgement

This research is funded by Vietnam National University Ho Chi Minh city (VNU-HCM) under grant number B2018-20b-01. We acknowledge the support time and facilities from Ho Chi Minh University of Technology (HCMUT), VNU-HCM; Laboratory of Advance Design and Manufacturing Processes, HCMUT; National Key Lab. of Digital Control and System Engineering (DCSELAB), HCMUT for this study.

## References

- Cao, J., Su, Y., Zhao, J., 2011. Design of an adaptive controller for dive-plane control of a torpedo-shaped AUV. *J. Mar. Sci. Appl.* 10 (3), 333–339. <https://doi.org/10.1007/s11804-011-1077-y>.
- Eichhorn, M., Ament, C., Jacobi, M., Pfuetzenreuter, T., Karimanzira, D., Bley, K., Boer, M., Wehde, H., 2018. Modular AUV system with integrated real-time water quality analysis. *Sensors* 18 (6), 1837. <https://doi.org/10.3390/s18061837>.
- Fossen, T., 1994. *Guidance and Control of Ocean Vehicles*. Wiley, NY, USA.
- Gharesi, N., Ebrahimi, Z., Forouzandeh, A., Areifi, M.M., 2017. Extended state observer-based backstepping control for depth tracking of the underactuated AUV. In: 2017 5th International Conference on Control, Instrumentation, and Automation (ICCIA), 2018-Janua, pp. 354–358. <https://doi.org/10.1109/ICCIautom.2017.8258706>.
- Hagen, P.E., Storkersen, N., Vestgard, K., Kartvedt, P., 2003. The HUGIN 1000 autonomous underwater vehicle for military applications. *Oceans 2003. Celebrating the Past .... Teaming Toward the Future* (IEEE Cat. No.03CH37492) 2 (2007), 1141–1145. <https://doi.org/10.1109/OCEANS.2003.178504>.
- Hong, E.Y., Soon, H.G., Chitre, M., 2010. Depth Control of an Autonomous Underwater Vehicle, STARFISH. OCEANS'10 IEEE SYDNEY, pp. 1–6. <https://doi.org/10.1109/OCEANSSYD.2010.5603566>.
- Jalving, B., 1994. The NDRE-AUV flight control system. *IEEE J. Ocean. Eng.* 19 (4), 497–501. <https://doi.org/10.1109/48.338385>.
- Joe, H., Kim, M., Yu, S., 2014. Second-order sliding-mode controller for autonomous underwater vehicle in the presence of unknown disturbances. *Nonlinear Dynam.* 78 (1), 183–196. <https://doi.org/10.1007/s11071-014-1431-0>.
- Khalil, H., 2002. *Nonlinear Systems*. Prentice Hall PTR.
- Lapierre, L., 2009. Robust diving control of an AUV. *Ocean Eng.* 36 (1), 92–104. <https://doi.org/10.1016/j.oceaneng.2008.10.006>.
- Liceaga-Castro, E., van der Molen, G.M., 1995. Submarine H/sup infinity/depth control under wave disturbances. *IEEE Trans. Contr. Syst. Technol.* 3 (3), 338–346. <https://doi.org/10.1109/87.406981>.
- Mahapatra, S., Subudhi, B., 2018. Design and experimental realization of a backstepping nonlinear H<sub>∞</sub> control for an autonomous underwater vehicle using a nonlinear matrix inequality approach. *Trans. Inst. Meas. Contr.* 40 (11), 3390–3403. <https://doi.org/10.1177/0142331217721315>.
- Mahapatra, S., Subudhi, B., Rout, R., Kumar, B.V.S.S.K., 2016. Nonlinear H<sub>∞</sub> control for an autonomous underwater vehicle in the vertical plane. *IFAC-PapersOnLine* 49 (1), 391–395. <https://doi.org/10.1016/j.ifacol.2016.03.085>.
- Mandal, K., Banerjee, T., Panja, A., 2019. Autonomous underwater vehicles: recent developments and future prospects. *Int. J. Res. Appl. Sci. Eng. Technol.* 7 (11), 215–222. <https://doi.org/10.22214/ijraset.2019.11036>.
- Moreira, L., Soares, C., 2008. \$H\_{\infty}\$ and \$H\_{\infty}\$ designs for diving and course control of an autonomous underwater vehicle in presence of waves. *IEEE J. Ocean. Eng.* 33 (2), 69–88. <https://doi.org/10.1109/JOE.2008.918689>.

- Naik, M.S., Singh, S.N., 2007. State-dependent Riccati equation-based robust dive plane control of AUV with control constraints. *Ocean. Eng.* 34 (11–12), 1711–1723. <https://doi.org/10.1016/j.oceaneng.2006.10.014>.
- Newman, J.N., 1977. In: *Marine Hydrodynamics*, first ed. MIT Press, Cambridge.
- Petricich, J., Stilwell, D.J., 2011. Robust control for an autonomous underwater vehicle that suppresses pitch and yaw coupling. *Ocean. Eng.* 38 (1), 197–204. <https://doi.org/10.1016/j.oceaneng.2010.10.007>.
- Presterro, T., 2001. Verification of a six-degree of freedom simulation model for the REMUS autonomous underwater vehicle. Ph.D. Thesis. In: Massachusetts Institute of Technology.
- Qiao, L., Ruan, S., Zhang, G., Zhang, W., 2018. Robust H<sub>2</sub> optimal depth control of an autonomous underwater vehicle with output disturbances and time delay. *Ocean. Eng.* 165, 399–409. <https://doi.org/10.1016/j.oceaneng.2018.07.019>.
- Rout, R., Subudhi, B., 2017. NARMAX self-tuning controller for line-of-sight-based waypoint tracking for an autonomous underwater vehicle. *IEEE Trans. Contr. Syst. Technol.* 25 (4), 1529–1536. <https://doi.org/10.1109/TCST.2016.2613969>.
- Silvestre, C., Pascoal, A., 2007. Depth control of the INFANTE AUV using gain-scheduled reduced order output feedback. *Contr. Eng. Pract.* 15 (7), 883–895. <https://doi.org/10.1016/j.conengprac.2006.05.005>.
- Sname, 1950. *Nomenclature for Treating the Motion of A Submerged Body through A Fluid*. Technical Report Bulletin 1-5. Society of Naval Architects and Marine Engineers, NY, USA.
- Tanakitkorn, K., Wilson, P.A., Turnock, S.R., Phillips, A.B., 2017. Depth control for an over-actuated, hover-capable autonomous underwater vehicle with experimental verification. *Mechatronics* 41 (3), 67–81. <https://doi.org/10.1016/j.mechatronics.2016.11.006>.
- Tran, N.H., Huynh, T.D., Ton, T.P., Huynh, T.H., 2019. Design of depth control for hybrid AUV. In: Proceedings of the 6th International Conference on Advanced Engineering - Theory and Applications 2019. Bogotá, Colombia.
- Wadoo, S.A., Sapkota, S., Chagachagere, K., 2012. Optimal control of an autonomous underwater vehicle. In: 2012 IEEE Long Island Systems, Applications and Technology Conference (LISAT), vol. 3, pp. 1–6. <https://doi.org/10.1109/LISAT.2012.6223100>.
- Wei, C., Yanhui, W., Jianhui, Z., 2015. Back-stepping control of underactuated AUV's depth based on nonlinear disturbance observer. In: 2015 34th Chinese Control Conference (CCC), 2015-Septe, pp. 6061–6065. <https://doi.org/10.1109/ChiCC.2015.7260587>.
- Wynn, R.B., Huvenne, V.A.I., Le Bas, T.P., Murton, B.J., Connelly, D.P., Bett, B.J., Ruhl, H.A., Morris, K.J., Peakall, J., Parsons, D.R., Sumner, E.J., Darby, S.E., Dorrell, R.M., Hunt, J.E., 2014. Autonomous Underwater Vehicles (AUVs): their past, present and future contributions to the advancement of marine geoscience. *Mar. Geol.* 352, 451–468. <https://doi.org/10.1016/j.margeo.2014.03.012>.
- Yan, Z., Yu, H., Hou, S., 2016. Diving control of underactuated unmanned undersea vehicle using integral-fast terminal sliding mode control. *J. Cent. S. Univ.* 23 (5), 1085–1094. <https://doi.org/10.1007/s11771-016-0358-7>.
- Yu, J., Liu, J., Wu, Z., Fang, H., 2018. Depth control of a bioinspired robotic dolphin based on sliding-mode fuzzy control method. *IEEE Trans. Ind. Electron.* 65 (3), 2429–2438. <https://doi.org/10.1109/TIE.2017.2745451>.
- Zhang, F., Marani, G., Smith, R.N., Choi, H.T., 2015. Future trends in marine robotics [TC spotlight]. *IEEE Robot. Autom. Mag.* 22 (1), 14–122. <https://doi.org/10.1109/MRA.2014.2385561>.